

LBL-7291
UC-32
TID-4500-R66

C-2

A HIGH ORDER FINITE ELEMENT METHOD FOR THE
CALCULATION OF CAPILLARY SURFACES

Robert A. Brown

December 1977

RECEIVED
LAWRENCE
BERKELEY LABORATORY

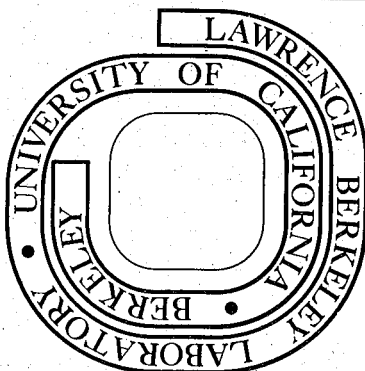
MAY 18 1978

LIBRARY AND
DOCUMENTS SECTION

Prepared for the U. S. Department of Energy
under Contract W-7405-ENG-48

TWO-WEEK LOAN COPY

*This is a Library Circulating Copy
which may be borrowed for two weeks.
For a personal retention copy, call
Tech. Info. Division, Ext. 6782*



LBL-7291

C-2

— LEGAL NOTICE —

This report was prepared as an account of work sponsored by the United States Government. Neither the United States nor the Department of Energy, nor any of their employees, nor any of their contractors, subcontractors, or their employees, makes any warranty, express or implied, or assumes any legal liability or responsibility for the accuracy, completeness or usefulness of any information, apparatus, product or process disclosed, or represents that its use would not infringe privately owned rights.

A HIGH ORDER FINITE ELEMENT METHOD
FOR THE CALCULATION OF CAPILLARY SURFACES

Robert A. Brown

Department of Chemical Engineering and Materials Science
University of Minnesota
Minneapolis, MN 55455*

December 1977

*Work performed under the auspices of the Department of Energy while the author was visiting at Lawrence Berkeley Laboratory.

ABSTRACT

A reduced quadratic finite element method on quadrilaterals is developed for discretizing the capillary equation in regular and irregular domains. Newton's method is used to solve the resulting set of nonlinear equations for the capillary surface. Numerical experiments are conducted for square and elliptical capillaries in order to compare this high order method to a bilinear finite element-Newton scheme and a finite difference - dynamic alternating direction implicit (DADI) technique. The reduced quadratic finite element method is shown to be the most efficient in these tests due to the relatively coarse element grids that can be used for accurate approximations.

INTRODUCTION

A numerical algorithm for the solution of a nonlinear elliptic partial differential equation can be characterized in terms of the discretization used to approximate the solution and the iteration technique used to solve the resulting nonlinear equation set. Finite difference methods are traditionally used for discretization. Finite element techniques are gaining popularity. Methods for solving nonlinear equations such as Newton's method, secant method, and successive approximations yield linear equation sets at each iteration and can be further classified by the technique, either direct or iterative, that is used to solve these systems.

We report here on a finite element - Newton method employing direct matrix techniques for the numerical solution of the Young-Laplace equation, the nonlinear elliptic partial differential equation governing the shape of a capillary surface. The method differs from earlier finite element approximations to this problem (1,2) in that here a high order accurate reduced quadratic basis function is used instead of the more easily formulated linear approximation. Three variants of Newton's method were tested for solution of the nonlinear finite element equations: (I) the standard Newton's procedure where the Jacobian matrix J is formulated at each iteration, (II) simplified Newton's iteration in which J is formed only initially, and (III) a hybrid method that combines the desirable features of both (I) and (II). Direct symmetric factorization was used to solve the linear equation sets in all three methods.

Since few analytical convergence estimates for the capillary problem are known empirical estimates must be inferred from computational experiments. We compare the reduced quadratic finite element approximation to a similar finite element formulation using bilinear basis functions and also to a finite difference approximation using the newly developed dynamic alternating direction

implicit method. The problems used as the basis of this comparison are the calculations of zero gravity capillary surfaces in square and elliptical cross-section capillaries. In the first geometry, the domain is regular and an analytical solution is known. No solution is known for the elliptical domain.

PROBLEM STATEMENT

The position of the interface between two static liquids inside a vertical, cylindrical capillary of arbitrary cross-section \mathcal{D} is given by the Young-Laplace equation, the nonlinear elliptic partial differential equation which relates the interface's location and mean curvature. For an interface represented in rectangular cartesian coordinates $z = z(x,y)$ the dimensionless equation is

$$-\nabla_{II} \cdot \tilde{N} = -\nabla_{II} \cdot \frac{k - z \tilde{i} - z \tilde{j}}{\sqrt{1 + z_x^2 + z_y^2}} = Bz(x,y) + \lambda \quad [1]$$

where \tilde{N} is the unit vector field everywhere normal to the interface and $\nabla_{II} = \frac{\partial}{\partial x} \tilde{i} + \frac{\partial}{\partial y} \tilde{j}$. The constants B and λ are the Bond number ($\Delta\rho g L^2 / \sigma$) and the dimensionless reference curvature ($2H_0 L / \sigma$), respectively, where $\Delta\rho$ is the density difference between the two liquids, g the gravitational constant, σ the interfacial tension, H_0 the reference mean curvature (evaluated at zero elevation) and L a reference length.

The interface meets the walls of the capillary at a given contact angle θ_c . In terms of \tilde{n}_s , the outward directed unit normal to the solid wall, the contact angle condition is

$$\tilde{N} \cdot \tilde{n}_s = \cos \theta_c \quad [2]$$

on the wall, $\partial\mathcal{D}$.

When the effects of gravity can be neglected ($B=0$), eq. [1] describes a surface of constant mean curvature λ . The calculations reported here are restricted to this case. Using a simple force balance (constructed by integrating eq. [1] over the capillary's cross-section) the mean curvature of the interface, the contact angle, and the geometry of the capillary can be related as

$$\lambda = \frac{L}{A} \cos \theta_c \quad [3]$$

where L is the perimeter of the capillary and A its cross-sectional area. Equation [3] is a necessary condition for the existence of an equilibrium capillary surface. In the absence of a gravitational field the solutions to eqs. [1-2] are invariant to translation in the z -coordinate; therefore, to uniquely specify the capillary surface one point on its surface must be fixed in space. For the capillaries shown in Figure 1 the surface height at the origin $(0,0)$ was set to zero.

The two geometries considered here are the square and elliptical capillaries (see Figure 1). For both configurations the existence of surfaces of constant mean curvature everywhere satisfying eq. [2] is possible only in a range of contact angles $90^\circ \geq \theta_c \geq \theta_{crit}$. Concus and Finn (3) have developed bounds for θ_{crit} which are tabulated for the square and elliptical cross-section capillaries in (4).

GALERKIN FINITE ELEMENT METHOD

The capillary problem eqs. [1-2] was discretized using the Galerkin finite element method. The domain was divided into quadrilateral sub-domains or elements on which a set of low order polynomial basis or trial functions was defined. The solution to eqs. [1-2] was approximated as a sum of these basis functions multiplied by unknown coefficients which were determined by setting the Galerkin weighted residuals to zero.

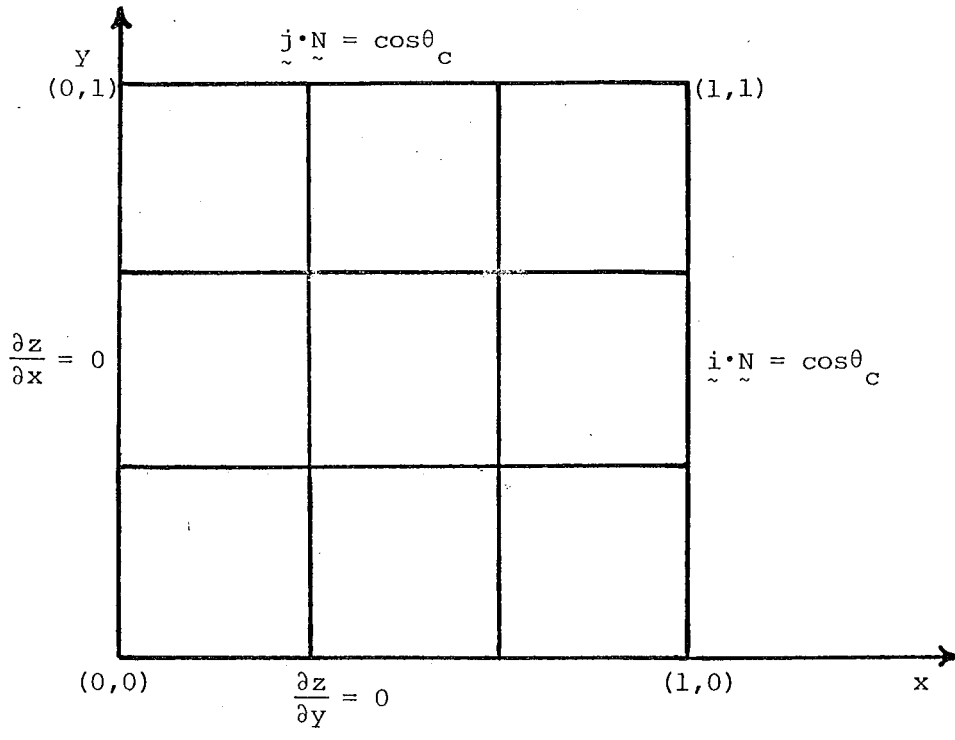


Figure 1a. Computational domain for square capillary. Contact angle and symmetry boundaries are shown.

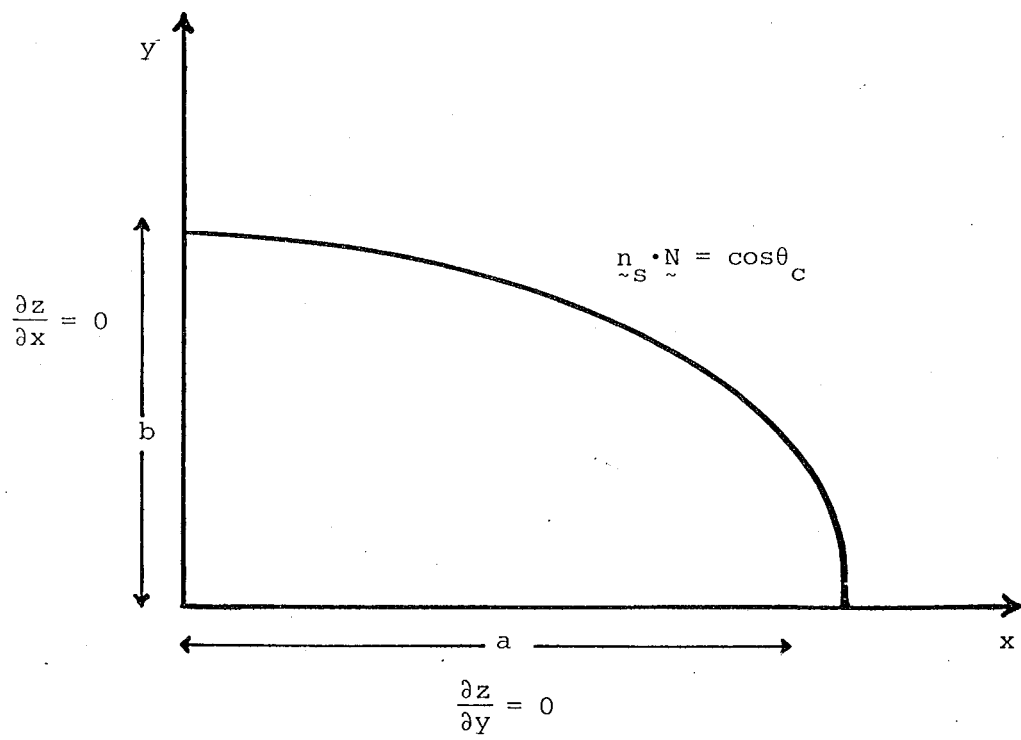


Figure 1b. Computational domain for elliptical capillary. Ratio of minor to major semi-axes is b/a. Contact angle and symmetry boundaries are shown.

Both Lagrangian bilinear and reduced quadratic elements (5) were studied. As in (6), the basis functions, $\Phi^i(\xi, \eta)$, were defined on the unit square E (see Figure 2) in terms of transformed coordinates (ξ, η) . The four Lagrangian bilinear basis functions on E

$$\Phi_{(E)}^i = a_{(E)}^i + b_{(E)}^i \xi + c_{(E)}^i \eta + d_{(E)}^i \xi \eta \quad i = 1, 3, 6, 8 \quad [4]$$

are determined in terms of the element's four vertices by

$$\Phi_{(E)}^i(\xi_j, \eta_j) = \delta_{ij} \quad i, j = 1, 3, 6, 8 \quad [5]$$

The reduced quadratic basis functions are defined at the four mid-side nodes as well as the vertices. These eight basis functions are of the form

$$\Phi_{(E)}^i = a_{(E)}^i + b_{(E)}^i \xi + c_{(E)}^i \eta + d_{(E)}^i \xi \eta + e_{(E)}^i \xi^2 + f_{(E)}^i \eta^2 + g_{(E)}^i \xi^2 \eta + h_{(E)}^i \xi \eta^2 \quad [6]$$

with the coefficients defined by

$$\Phi_{(E)}^i(\xi_j, \eta_j) = \delta_{ij} \quad i, j = 1, \dots, 8 \quad [7]$$

The basis functions on an element (e) (see Figure 2) in the domain are related to the basis functions on the unit square (E) by

$$\Phi_{(e)}^i(x, y) = \Phi_{(E)}^i(\xi(x, y), \eta(x, y)) \quad \begin{cases} i = 1, 3, 6, 8 \text{ bilinear functions} \\ i = 1, \dots, 8 \text{ reduced biquadratic} \\ \text{functions} \end{cases} \quad \text{in (e)} \quad [8]$$

$$\Phi_{(e)}^i = 0 \quad \text{outside (e)}$$

where the mapping from (E) to (e) is given by the transformation

$$\begin{aligned} x &= \sum_{\substack{\text{all } i \\ \text{in (E)}}} \Phi_{(E)}^i(\xi, \eta) x_i \\ y &= \sum_{\substack{\text{all } i \\ \text{in (E)}}} \Phi_{(E)}^i(\xi, \eta) y_i \end{aligned} \quad [9]$$

and (x_i, y_i) are the nodal coordinates on (e). The solution of eqs. [1-2] is

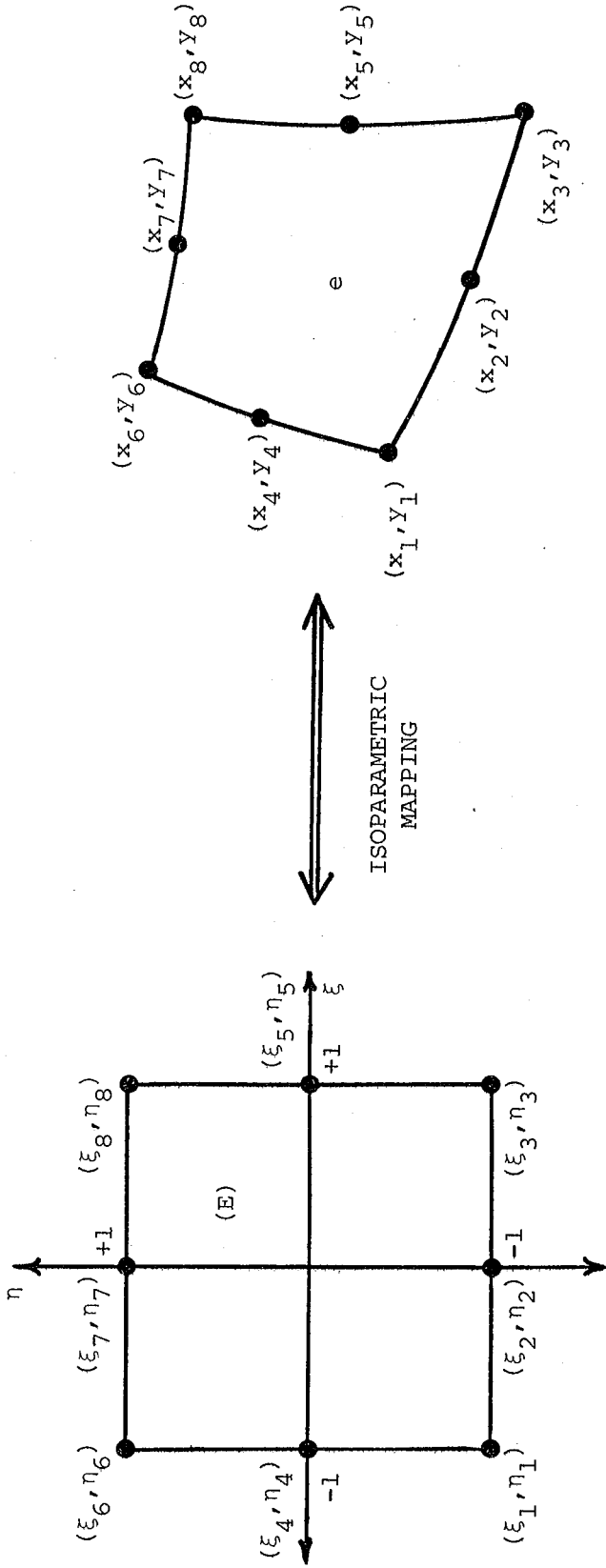


Figure 2. Relationship between unit element (E) in transformed coordinates (ξ, η) and an element (e) in the computational domain for eight point reduced quadratic element.

approximated within each element of \mathcal{D} as

$$z(x,y) = \sum_{\substack{\text{all } i \\ \text{in } (\mathbb{E})}} \alpha_i \Phi_i^i(x,y) \quad \text{in}(e) \quad [10]$$

where the coefficients $\{\alpha_i\}$ are determined by forcing the Galerkin weighted residuals of eq. [1] to zero, i.e.,

$$\int_{\mathcal{D}} \Phi_i^i(e) \left\{ \nabla_{II} \cdot \vec{N} + Bz + \lambda \right\} da = 0 \quad i = 1, \dots, \mathcal{N}. \quad [11]$$

The total number of basis functions in the domain is \mathcal{N} . Integrating eq. [11] by parts and applying the divergence theorem gives

$$\int_{\mathcal{D}} \left\{ \Phi_i^i(e) (Bz + \lambda) - \nabla \Phi_i^i(e) \cdot \vec{N} \right\} da + \oint_{\partial \mathcal{D}} \Phi_i^i(e) \vec{n}_s \cdot \vec{N} ds = 0 \quad i = 1, \dots, \mathcal{N}. \quad [12]$$

The domain's boundary $\partial \mathcal{D}$ can be divided into two parts: 1) the portion of the boundary $\partial \mathcal{D}_{\text{SOLID}}$ on which the contact angle boundary condition ($\vec{n}_s \cdot \vec{N} = \cos \theta_c$) holds and 2) the boundary $\partial \mathcal{D}_{\text{SYM}}$ on which a symmetry condition ($\vec{n}_s \cdot \vec{N} = 0$) is specified. See Figure 1. Making these substitutions in the residual eqs. [12] incorporates the boundary conditions as

$$R^i(\underline{\alpha}) = \int_{\mathcal{D}} \left\{ \Phi_i^i(e) (Bz + \lambda) - \nabla \Phi_i^i(e) \cdot \vec{N} \right\} da + \cos \theta_c \oint_{\partial \mathcal{D}_{\text{SOLID}}} \Phi_i^i(e) ds = 0 \quad i = 1, \dots, \mathcal{N}. \quad [13]$$

It is not completely fortuitous that the boundary conditions blend easily into the Galerkin residuals. These boundary conditions are the natural conditions for eq. [1]; eq. [13] is the same result as obtained from a variational or energy minimization formulation of the capillary problem (see (5)).

Using the definition of \vec{N} given in eq. [1], eq. [13] becomes

$$R^i(\underline{\alpha}) = \int_{\mathcal{D}} \left\{ \Phi_i^i(e) (Bz + \lambda) + \frac{\Phi_i^i(e) x z_x + \Phi_i^i(e) y z_y}{\sqrt{1 + z_x^2 + z_y^2}} \right\} da + \cos \theta_c \oint_{\partial \mathcal{D}_{\text{SOLID}}} \Phi_i^i(e) ds = 0 \quad [14]$$

$i = 1, \dots, \mathcal{N}$

which, once the solution expansion eq. [10] is introduced, is recognized as a nonlinear equation set for $\{\alpha_i\}$. The integrals in eq. [14] were approximated using nine point Gaussian integration.

SOLUTION OF FINITE ELEMENT EQUATIONS

The three methods tested for solving the nonlinear equation set [14] were full Newton, simplified Newton, and hybrid Newton iterations. The full Newton's method (FNM) calculates the new (k+1)st iterate for the unknowns $\{\alpha_i^{(k+1)}\}$ from the kth iterate as

$$\alpha^{(k+1)} = \alpha^{(k)} - \underline{J}^{-1}(\alpha^{(k)}) \underline{R}(\alpha^{(k)}) = \alpha^{(k)} - \delta^{(k)} \quad [15]$$

where the Jacobian matrix ($J_{ij} = \partial R_i / \partial \alpha_j$) is the local gradient of the residuals with respect to the unknown coefficients. This iteration is continued until the correction vector $\delta^{(k)}$ satisfies

$$\max_{i=1, \dots, n} |\delta_i^{(k)}| < \epsilon \quad [16]$$

At each iteration eq. [15] requires the formulation and solution of the linear equation system

$$\underline{J}^{(k)} \delta^{(k)} = \underline{R}^{(k)} \quad [17]$$

with

$$J_{ij}(\alpha^{(k)}) = \left\{ \frac{\phi^i(e)x^{\phi^j} + \phi^i(e)y^{\phi^j}}{\sqrt{1+z_x^2+z_y^2}} - \frac{(\phi^i(e)x^z_x + \phi^i(e)y^z_y)(\phi^j(e)x^z_x + \phi^j(e)y^z_y)}{\sqrt{1+z_x^2+z_y^2}} + B\phi^i(e)\phi^j(e) \right\} \Big|_{\alpha = \alpha^{(k)}} da \quad [18]$$

The matrix \underline{J} is symmetric, sparse, and banded. The bandwidth depends on the numbering scheme used for the nodes. Equation [17] was solved by factoring \underline{J} into $\underline{L} \underline{D} \underline{L}^T$ (\underline{L} is lower triangular and \underline{D} is diagonal) using the profile matrix storage technique as implemented in (6). The resulting triangular

equation systems were easily solved.

The simple Newton's method (SNM) requires only the formulation and factorization of the Jacobian matrix associated with the initial approximation $\{\alpha^{(0)}\}$. Successive iterates are calculated using this initial gradient approximation

$$\alpha^{(k+1)} = \alpha^{(k)} - J^{-1}(\alpha^{(0)}) R(\alpha^{(k)}) \quad [19]$$

Simple Newton's method requires at each iteration only the calculation of the residual vector $R(\alpha^{(k)})$ and the solution of the triangular systems

$$L(\alpha^{(0)}) D(\alpha^{(0)}) L^T(\alpha^{(0)}) \delta^{(k)} = R(\alpha^{(k)}) \quad [20]$$

Sherman (7) has imbedded SNM into a family of Newton-Richardson procedures where iterative solutions to the linear systems of equations generated by eq. [15] at each kth iteration are constructed at the expense of formulating $J(\alpha^{(k)})$. For the finite difference solution of the minimal surface equation, a problem of similar complexity to the one considered here, Sherman (7) found SNM the most efficient of the Newton-Richardson family. For mildly nonlinear minimal surfaces SNM was also more efficient than the full Newton's procedure.

The accuracy of the gradient approximation of the full Newton's method leads to accelerated convergence, at the expense of more computation, compared to the simple Newton's procedure where the gradient approximation is not updated. A hybrid Newton's method (HNM) was tested which after an initial full Newton iteration uses SNM iterations as long as the convergence factor $f^{(k+1)} = \|\delta^{(k+1)}\|_2 / \|\delta^{(k)}\|_2$ is smaller than a specified level f_0 , taken as 1/2 throughout this work. If during execution $f^{(k+1)}$ increases above f_0 , a new approximation to the Jacobian matrix is calculated, factored, and the iterations are continued.

TABLE 1. Execution times for full Newton
and simplified Newton iterations

Function	Time/Iteration (CPU sec)	
	Full Newton	Simple Newton
Form $\tilde{J}(\alpha^{(k)}), \tilde{R}(\alpha^{(k)})$.248	—
Form $\tilde{R}(\alpha^{(k)})$	—	.104
Factor \tilde{J}	.396	—
Solve eq. [20]	.042	.042
Total Time	.686	.146

TABLE 2. Results of comparison of full, simple and hybrid
Newton's methods for contact angles of 80, 40,
and 20°.

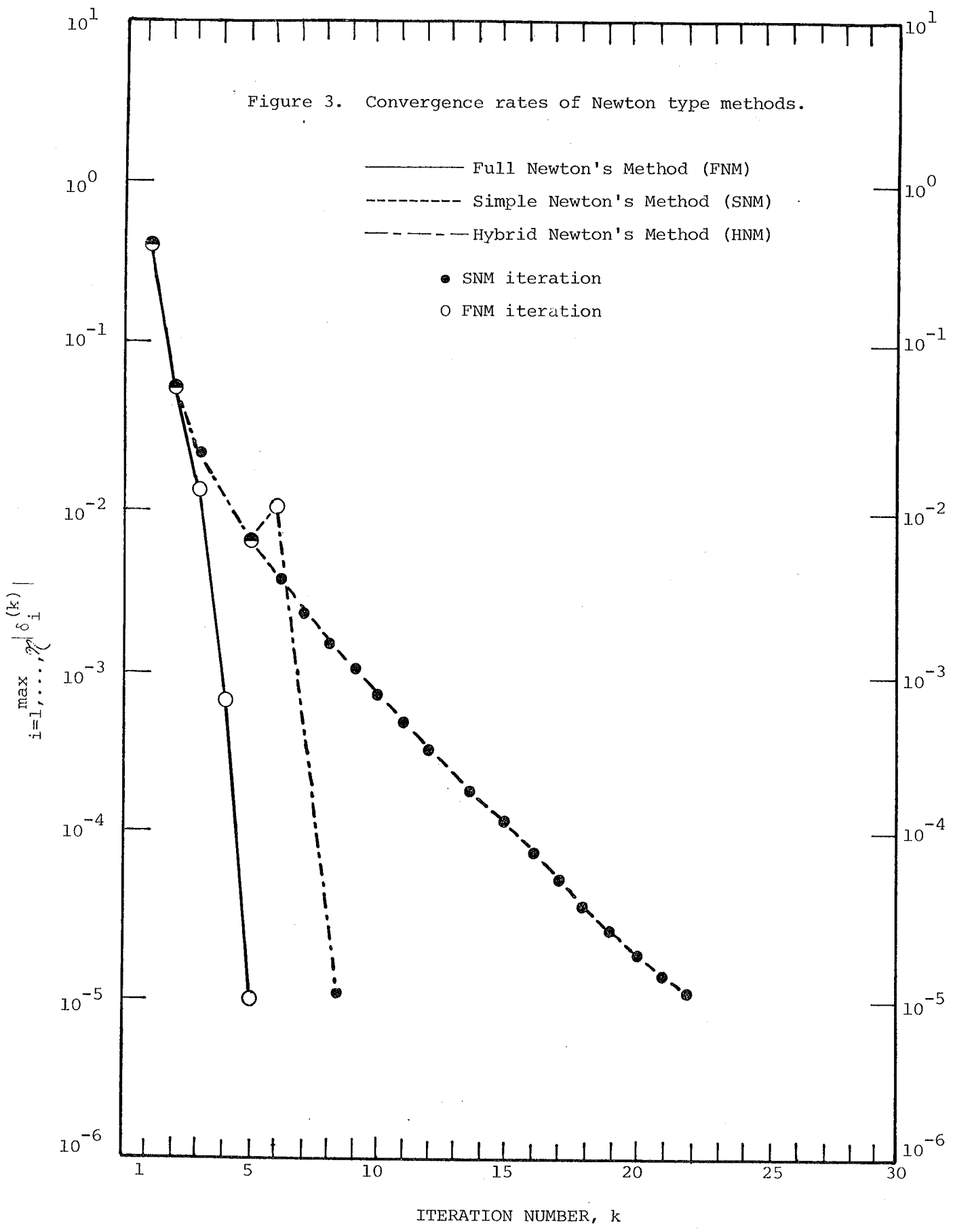
Iteration Method	θ_c	Number of Iterations		E	Total Execution Time (sec)
		NM	SNM		
HNM	80	1	2	1×10^{-5}	1.36
FNM	80	3	0	1×10^{-5}	2.28
SNM	40	1	21	1×10^{-5}	3.99
FNM	40	5	0	1×10^{-5}	3.64
HNM	40	3	12	1×10^{-5}	3.86
SNM	20	1	41	5×10^{-5}	6.78
FNM	20	7	0	1×10^{-5}	5.06
HNM	20	4	6	1×10^{-5}	3.83

The three iteration schemes, full Newton's method, SNM, and HNM, were compared for solving the nonlinear equation set [14] generated for the shape of a interface in an elliptical capillary ($a/b = .6$) with contact angles of 20, 40, and 80°. A grid of eight reduced quadratic elements in each direction (see Figure 3) was used for the calculations given in Table 2. The calculations were performed using the FTN4 compiler (OPT = 2) on the CDC 7600 computer at Lawrence Berkeley Laboratory. Timing estimates reported here are in central processor seconds. The execution times for iterations of SNM and FNM are summarized in Table 1. The factor of five increase in execution time of FNM over SNM can be attributed to the expense of factoring the Jacobian matrix.

The results of the comparison of the three Newton methods are tabulated in Table 2. For $\theta_c = 80^\circ$ where the interface is nearly flat, HNM reduces to SNM. Here the initially calculated Jacobian matrix is a good approximation for later iterations and SNM iterations converge quickly enough that the hybrid scheme need not update \tilde{J} . The SNM iteration is also more efficient than FNM as predicted by Sherman.

For contact angles of 40° and 20°, the initial Jacobian matrix is no longer a good approximation for later iterations; SNM converges very slowly (see Figure 3) and is inefficient when compared to either FNM or HNM. The hybrid scheme is the most efficient of the three procedures. The reason for HNM's success is clearly seen in Figure 3 where the maximum change in the Newton's correction vector per iteration is plotted. The hybrid scheme follows SNM as long as the convergence rate is acceptable ($f^{(k+1)} < f_0$). When the convergence rate becomes slow ($k = 6$ in Figure 3) the Jacobian matrix is recomputed and the SNM iteration is diverted down a faster converging path.

Figure 3. Convergence rates of Newton type methods.



COMPUTATIONAL EXPERIMENTS

Finite element programs solving the capillary equation in the square and elliptical geometries were developed for comparison of the bilinear and reduced quadratic elements and comparison with the finite difference - dynamic alternating direction implicit method (DADI) developed by Doss (6). All programs were coded in FORTRAN IV. This report includes results run on both the CDC 7600 computer of Lawrence Berkeley Laboratory and the CDC Cyber 74 at the University of Minnesota with the FTN4 (OPT = 2) compiler used at both installations. No attempt has been made to compare results from the two machines.

The results that follow are divided into two parts: 1) comparisons for the square capillary tube where an exact solution is known, and 2) results for the irregular elliptical domain. All calculations were performed using a flat interface as the initial guess ($\alpha^{(0)} = 0$) for the capillary surface.

Square Capillary

Equations [1-2] were solved on a domain consisting of one quadrant of the total cross-section of the square capillary (see Figure 1). In this geometry, a simple, closed form solution exists: for $45^\circ \leq \theta_c \leq 90^\circ$ the capillary surface is given as a piece of sphere of radius $1/\lambda$. For contact angles below 45° no solution exists for Eqs. [1-2].

The accuracy and efficiency of the bilinear and reduced quadratic basis functions for the solution of Eqs. [1-2] on the square were compared using the element grids summarized in Table 3 where \mathcal{N} is the total number of basis functions in the domain and h is the element size. The hybrid Newton's method (HNM) discussed above was used to solve the nonlinear residual equations. The iterations were continued until the largest change in the correction vector $\delta^{(k)}$ was less than 10^{-5} (see Eq. [16]).

TABLE 3. Meshes used in the comparison of bilinear and reduced quadratic finite elements.

<u>Mesh</u>	<u>Basis Function</u>	<u>Elements</u>	<u>\mathcal{N}</u>	<u>h</u>
L8	bilinear	8×8	81	.125
L16	bilinear	16×16	289	.0625
L32	bilinear	32×32	1089	.03125
Q8	reduced quad.	8×8	225	.125
Q16	reduced quad.	16×16	833	.0625

The capillary surface's location, the exact solution and percent relative error at the points (0,1) and (1,1) are given in Table 4 for contact angles of 80, 50, and 45°. Also shown are the approximate contact angles calculated from the finite element solution and eq. [2]. At $\theta_c = 80^\circ$, both bilinear and reduced quadratic basis functions give accurate approximations to the capillary surface location and contact angle. In most of these cases the solution error is of the same order as the convergence criterion (10^{-5}).

For the lower contact angles the capillary surface becomes more curved and the bilinear basis functions cannot effectively interpolate the surface when grids such as L8 and even L16 are used. On the other hand, the reduced quadratic basis functions on a coarse grid (Q8) give solutions and contact angles that are more accurate than even the 32×32 bilinear approximation (L32). The high accuracy of the reduced quadratic approximation for a small number of elements results in a high computational efficiency for the high order element.

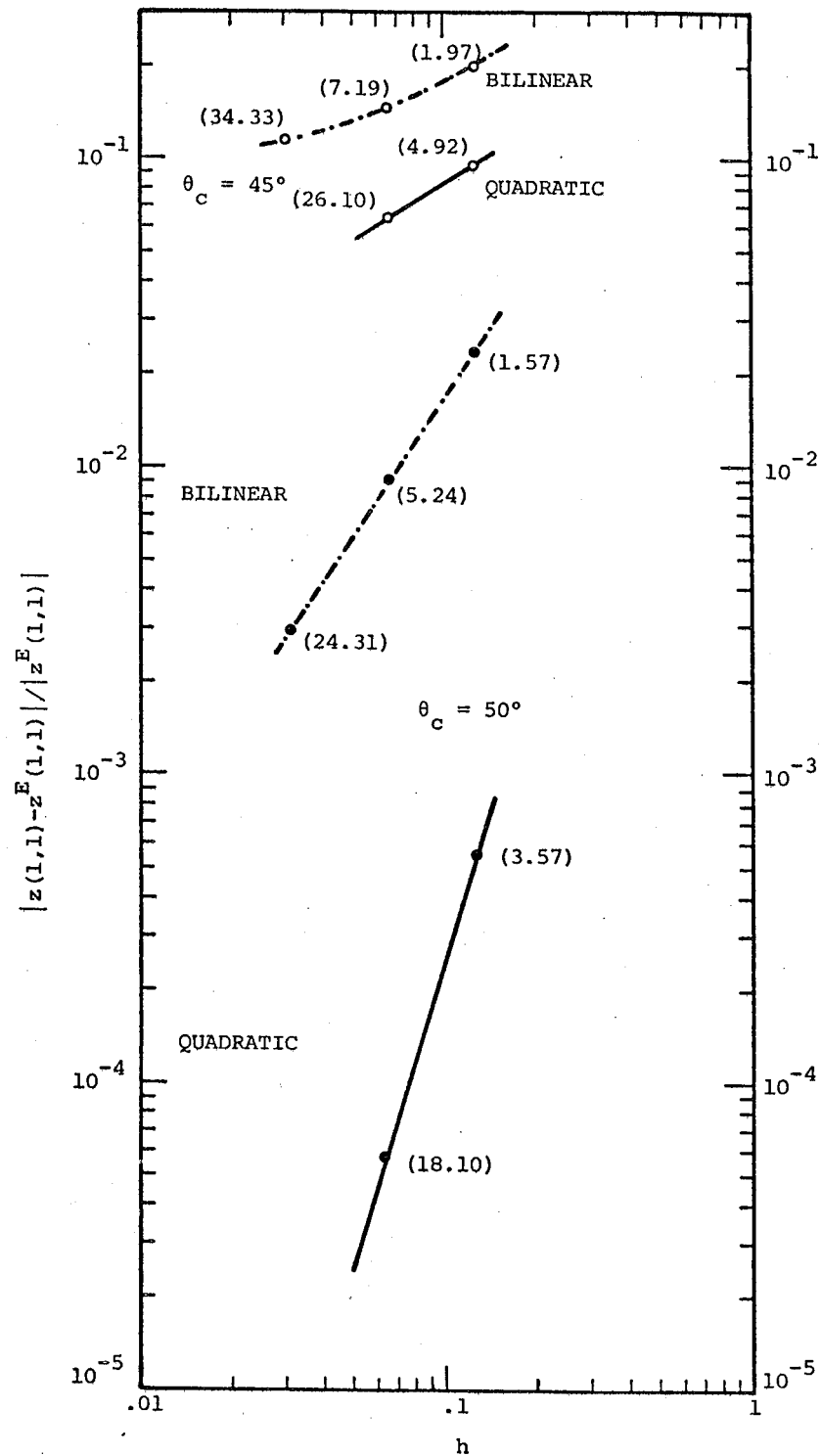
Figure 4 shows the strong dependence of the error in the finite element approximation at (1,1) on the contact angle. This is not totally unexpected. As the contact angle is decreased, the height of the capillary surface and its slopes at (1,1) become very large thus causing a large error in a discretized

TABLE 4. Comparison of bilinear and reduced quadratic finite element methods for capillary problem on a square. Contact angles of 80, 50, and 45° are listed.

	θ_c	$z(0,1)$	$z^E(0,1)$	Relative Error (%)	$\tilde{\theta}_c(0,1)$	$z(1,1)$	$z^E(1,1)$	Relative Error (%)	$\tilde{\theta}_c(1,1)$	Execution Times (sec)*
L8	80	0.08748	0.08749	0.005	80.63	.17630	.17635	0.026	80.64	0.94
L16	80	0.08749	0.08749	—	80.32	.17634	.17635	0.007	80.32	2.57
L32	80	0.08749	0.08749	—	80.16	.17634	.17635	0.002	80.16	10.35
Q8	80	0.08749	0.08749	—	80.00	.17635	.17635	—	80.00	1.73
Q16	80	0.08749	0.08749	—	80.00	.17635	.17635	—	80.00	6.98
L8	50	.36360	.36397	0.102	52.96	.88606	.90744	2.356	54.17	1.57
L16	50	.36389	.36397	0.026	51.49	.89926	.90744	0.901	52.35	5.24
L32	50	.36395	.36397	0.006	50.75	.90480	.90744	0.290	50.89	24.31
Q8	50	.36397	.36397	—	50.11	.90695	.90744	0.054	50.24	3.57
Q16	50	.36397	.36397	0.006	50.03	.90738	.90744	0.006	50.07	18.10
L8	45	0.41368	0.41421	0.130	48.49	1.14221	1.41421	19.233	51.28	1.97
L16	45	0.41408	0.41421	—	46.76	1.20474	1.41421	14.812	49.28	7.19
L32	45	0.41418	0.41421	0.033	45.89	1.25146	1.41421	11.508	47.94	34.33
Q8	45	0.41421	0.41421	—	45.18	1.27935	1.41421	9.536	45.90	4.92
Q16	45	0.41421	0.41421	—	45.05	1.31866	1.41421	6.756	45.45	26.10

*Times taken on the CDC CYBER 74, University of Minnesota

Figure 4. Convergence rates of bilinear (—•—) and reduced quadratic (—) finite element approximations for the height of a meniscus in a square capillary. Results for contact angles of 50 and 45 degrees are shown with computation times on University of Minnesota Cyber 74 given in parenthesis.



approximation. The convergence proof of Mittleman (7) for the finite element solution of eq. [1-2] using linear basis functions in a capillary with a smooth boundary shows that an integrated measure of the error will not be as sensitive to contact angle.

The reduced quadratic finite element code was compared to the finite difference discretization of Concus (8) with the resulting set of nonlinear equations solved by the dynamic alternating direct implicit method of Doss (6). Uniform 20×20 (DADI20) and 40×40 (DADI40) finite difference grids from (9) were used in the results presented in Table 5. Again, as in the previous comparison of bilinear and reduced quadratic elements, the higher order finite element method is more efficient because of the relatively coarse grid needed for high accuracy.

The convergence rates of finite difference, bilinear, and reduced quadratic finite element methods are plotted versus h , the grid or element size, on Figure 5. The finite difference and bilinear finite element approximations exhibit similar rates of convergence; this is expected since both techniques reduce to $\mathcal{O}(h^2)$ approximations for linear problems (see (8) and (3)).

Elliptical Capillary

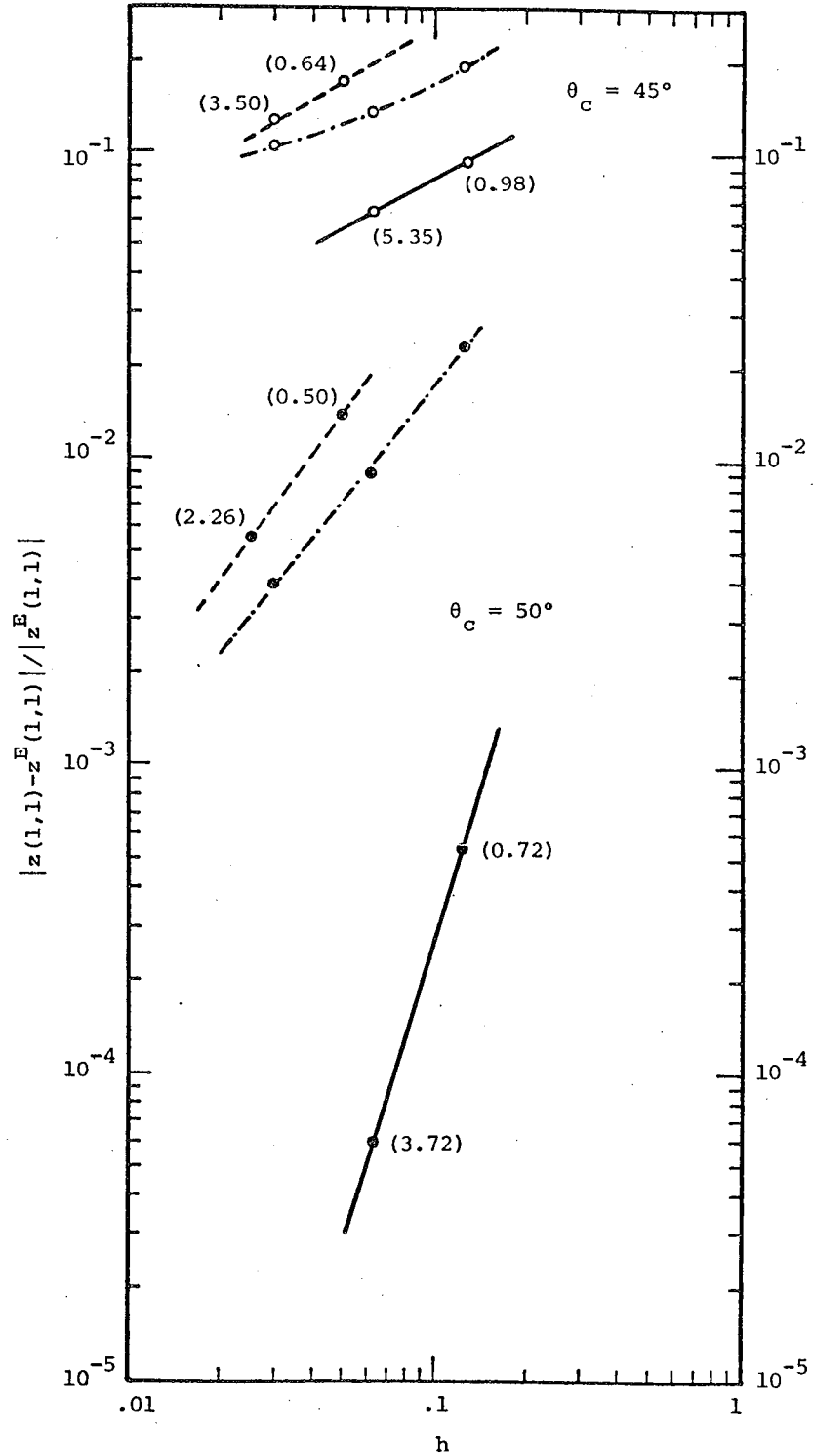
The reduced quadratic finite element method was formulated for the capillary problem on a quadrant of a capillary with elliptical cross-section (see Figure 1b). To construct a quadrilateral element mesh on this domain eqs. [1-2] were cast in terms of cylindrical polar coordinates $z = z(r, \theta)$. In this representation the domain becomes an irregular quadrilateral as shown in Figure 6 for $b/a = 0.6$. Note that the isoparametric mapping, eq. [9], gives a reduced quadratic interpolation for the boundary of the capillary.

TABLE 5. Comparison of reduced quadratic finite element method and finite difference-DADI technique for capillary problem on a square. Contact angles of 80, 50, and 45° are listed.

	θ_c	$z(0,1)$	$z^E(0,1)$	Relative Error (%)	$z(1,1)$	$z^E(1,1)$	Relative Error (%)	Execution Times (sec)*
DADI20	80	.08749	0.08749	—	0.17633	0.17635	0.011	0.44
DADI40	80	.08749	0.08749	—	0.17634	0.17635	0.006	1.80
Q8	80	.08749	0.08749	—	0.17634	0.17635	—	
DADI20	50	0.36412	0.36397	0.041	0.89467	0.90744	1.407	0.50
DADI40	50	0.36401	0.36397	0.011	0.90242	0.90744	0.553	2.26
Q8	50	0.36397	0.36397	—	0.90695	0.90744	0.054	0.74
Q16	50	0.36397	0.36397	—	0.90738	0.90744	0.006	3.72
DADI20	45	0.41449	0.41421	0.068	1.16890	1.41421	17.197	0.64
DADI40	45	0.41428	0.41421	0.017	1.21907	1.41421	13.799	3.50
Q8	45	0.41421	0.41421	—	1.27935	1.41421	9.536	0.98
Q16	45	0.41421	0.41421	—	1.31866	1.41421	6.756	5.35

*Times taken on the CDC 7600, Lawrence Berkeley Laboratory

Figure 5. Convergence rates of bilinear (—•—), reduced quadratic (—) finite element, and finite difference (---) approximations for the height of a meniscus in a square capillary. Results for contact angles of 50 and 45 degrees are shown with computation times on LBL CDC 7600 given in parenthesis.



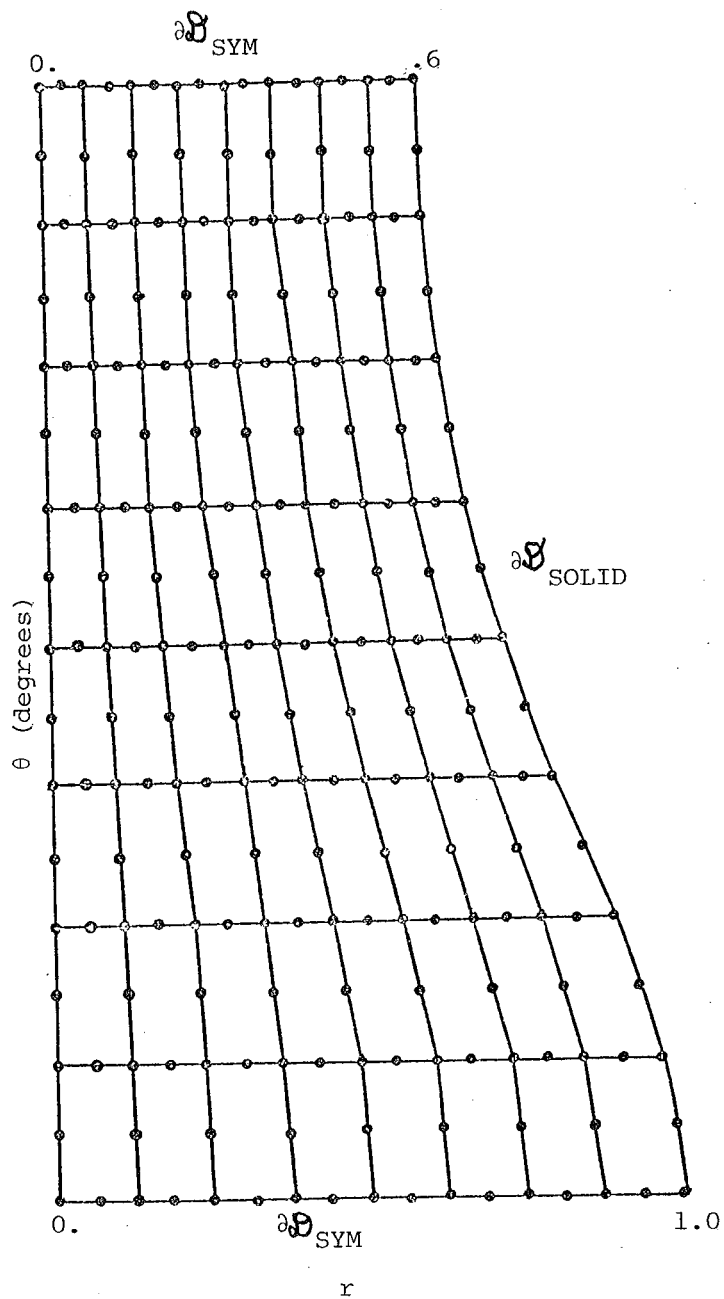


Figure 6. Cross-section of elliptical capillary in cylindrical polar coordinates. The ratio of minor to major semi-axes is .6.

The dependence of the surface's height on contact angle was studied and compared to the bilinear finite element calculations of Albright (4). The calculated heights at the intersections of the major and minor axes with the capillary wall are shown in Figure 7 for both a 16×16 reduced quadratic and Albright's 21×11 mesh. The relatively coarse mesh of the bilinear finite element formulation was necessary because of slow convergence of the block successive over relaxation-Newton's method used in (4) to solve the system of nonlinear equations. Note that for small contact angles, where the surface's slopes are large, the higher order method gives higher and probably more accurate values of the meniscus height than does the bilinear approximation.

The reduced quadratic finite element approximation was also compared to the finite difference-DADI scheme of Doss (11) for 41×41 (DADI41) and 101×101 (DADI101) grids. In the results shown in Table 6 the finite difference calculations consistently predicted capillary heights greater than those found by the high order finite element method. In the finite difference formulation the irregular domain has been replaced by a polygonal approximation: the corners introduced into the computational domain cause the calculated capillary heights to be greater than those for the true capillary. The quadratic boundary approximation used by the finite element technique all but eliminates this source of error.

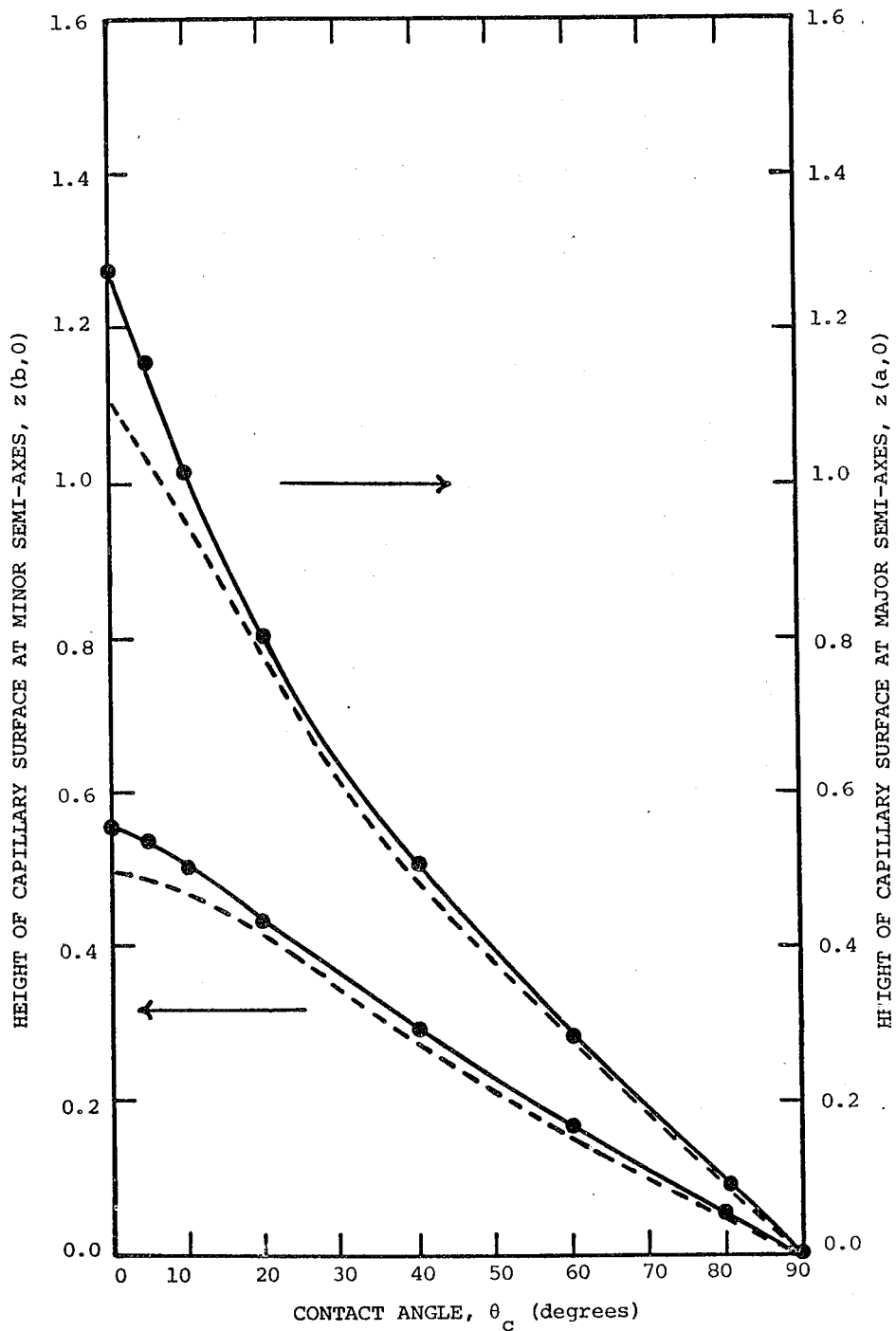


Figure 7. Dependence of capillary surface height on contact angle for elliptical cross-section capillary ($b/a = 0.6$). Heights of the surface at the intersection of the major and minor semi-axes and the wall are shown for 16×16 quadratic element mesh (—) and Albright's 21×11 linear element mesh.

TABLE 6. Comparison of reduced quadratic finite element and finite difference - DADI methods for capillary problem in an elliptical domain. Contact angles of 60, 20 and 10 are listed.

	θ_c ($^\circ$)	$z(a,0)$	$z(b,\pi/2)$	Execution Time (sec)*
DADI32	60	0.27564	0.16057	1.07
DADI64	60	0.27533	0.16056	4.65
Q8	60	0.27525	0.16052	0.58
Q16	60	0.27524	0.16055	2.69
DADI32	20	0.77727	0.40944	2.31
DADI64	20	0.77423	0.40857	11.97
Q8	20	0.77308	0.40761	0.94
Q16	20	0.77287	0.40814	4.94
DADI32	10	0.98491	0.48653	3.80
DADI64	10	0.98285	0.48330	19.00
Q8	10	0.97690	0.47638	1.02
Q16	10	0.98221	0.48011	5.47

*Times taken on the CDC 7600, Lawrence Berkeley Laboratory

Although no exact solution is known for an interface in an elliptical cross-section capillary, the respective accuracy of the two methods can be inferred through the effects of mesh refinement. Table 6 gives results for contact angles of 60, 20, and 10 degrees. For $\theta_c = 60^\circ$ both discretizations give accurate solutions with relatively coarse grids (DADI32 and Q8), with their solutions invariant to grid refinements (DADI64 and Q16). The results for 20 and 10 degrees show the evolution of both approximations with mesh refinement. The fine grids Q16 and DADI64 give similar solutions. The reduced quadratic finite element solutions, as in the square domain, require much less computation time than the very refined finite difference approximation. Also the convergence of the FEM-Newton method is not as sensitive to contact angle as the DADI method: the ratios of execution times of the 20 to the 10 degree cases are 1.1:1 and 1.6:1 respectively.

DISCUSSION

The reduced quadratic finite element-Newton's technique developed here for solving the nonlinear, elliptic Young-Laplace equation has been shown more efficient than a finite element-Newton scheme using bilinear basis functions and a finite difference method using a very efficient nonlinear iteration scheme (DADI). The efficiency of the high order finite element method results from the relatively coarse grids with which highly accurate solutions can be obtained. These small grids lead to small linear equation sets (n less than 1000) in the Newton's linearization and make the direct factorization technique employed here acceptable.

The loss of existence of the interface below a critical contact angle is an additional computational difficulty of capillary problems; optimally, any numerical simulation of these problems should mimic this behavior. As reported in (4), the bilinear finite element - BSOR method finds solutions to the discretized system of equations for angles well below θ_{crit} . Similar results were obtained with the finite difference - DADI technique (9). The high order finite element-Newton scheme failed to converge for contact angles much below θ_{crit} . For example: in the square capillary ($\theta_{crit} = 45^\circ$), solutions to the discretized problem were found only down to 44° . Since it is doubtful that the equation set fails to have a solution below this contact angle, the best explanation for such behavior is that the equation set becomes too ill-conditioned for the Newton's method to converge. The apparent loss of existence of the approximate solution is then tied to changes in the domain of convergence of the nonlinear iteration technique. More work is needed to fully understand this behavior.

ACKNOWLEDGEMENTS

The bulk of this work was done while the author was a visitor at Lawrence Berkeley Laboratory. The author is indebted to Paul Concus of LBL and L. E. Scriven of University of Minnesota, for their comments and suggestions during the course of this study. Thanks are also due to Said Doss for supplying the results from his finite difference-DADI technique. This work was partially supported through the University of Minnesota Computer Center and a Graduate School Dissertation Fellowship held by the author.

REFERENCES

- (1) Orr, F. M., Jr., Scriven, L. E., Rivas, A. P., Menisci in arrays of cylinders: numerical simulation by finite elements. J. Colloid Interface Sci. 52 602-610 (1975).
- (2) Orr, F. M., Jr., Brown, R. A., Scriven, L. E., Three-dimensional menisci: numerical simulation by finite elements. J. Colloid Interface Sci. 60 137-147 (1977).
- (3) Concus, P., Finn, R., On capillary-free surfaces in the absence of gravity. Acta Math. 177-198 (1974).
- (4) Albright, N., Numerical computation of capillary surfaces on irregularly shaped domains by a finite element method. Lawrence Berkeley Laboratory Report LBL-6136 (1977).
- (5) Strang, G., Fix, G. J., An Analysis of the Finite Element Method. Prentice-Hall, Englewood Cliffs, New Jersey (1973).
- (6) Bätke, K. J., Wilson, E. L., Numerical Methods in Finite Element Analysis. Prentice-Hall, Englewood Cliffs, New Jersey (1976).
- (7) Sherman, A. H., On the efficient solution of sparse systems of linear and nonlinear equations. Ph.D. thesis, Yale University (1975).
- (8) Doss, S., Dynamic ADI methods for elliptic equations with gradient dependent coefficients. LBL-6142 (1977).
- (9) Mittleman, H. D., On the approximation of capillary surfaces in a gravitational field. Computing 18 141-148 (1977).
- (10) Concus, P., Numerical solution of the minimal surface equation. Math. Comp. 21 340-350 (1967).
- (11) Doss, S., private communication. (Nov. 1977).

This report was done with support from the United States Energy Research and Development Administration. Any conclusions or opinions expressed in this report represent solely those of the author(s) and not necessarily those of The Regents of the University of California, the Lawrence Berkeley Laboratory or the United States Energy Research and Development Administration.

